Adaptation to direction statistics modulates perceptual discrimination

Nicholas S. C. Price
Department of Physiology, Monash University, Clayton, Victoria, Australia

Danielle L. Prescott
Department of Physiology, Monash University, Clayton, Victoria, Australia

Perception depends on the relative activity of populations of sensory neurons with a range of tunings and response gains. Each neuron's tuning and gain are malleable and can be modified by sustained exposure to an adapting stimulus. Here, we used a combination of human psychophysical testing and models of neuronal population decoding to assess how rapid adaptation to moving stimuli might change neuronal tuning and thereby modulate direction perception. Using a novel motion stimulus in which the direction changed every 10 ms, we demonstrated that 1,500 ms of adaptation to a distribution of directions was capable of modifying human psychophysical direction discrimination performance. Consistent with previous reports, we found perceptual repulsion following adaptation to a single direction. Notably, compared with a uniform adaptation condition in which all motion directions were equiprobable, discrimination was impaired after adaptation to a stimulus comprising only directions ± 30–60° from the discrimination boundary and enhanced after adaptation to the complementary range of directions. Thus, stimulus distributions can be selectively chosen to either impair or improve discrimination performance through adaptation. A neuronal population decoding model incorporating adaptation-induced repulsive shifts in direction tuning curves can account for most aspects of our psychophysical data; however, changes in neuronal gain are sufficient to account for all aspects of our psychophysical data.

Keywords: adaptation, motion, discrimination, decoding model

Citation: Price, N. S. C., & Prescott, D. L. (2012). Adaptation to direction statistics modulates perceptual discrimination. *Journal of Vision, 12*(6):32, 1–17, http://www.journalofvision.org/content/12/6/32, doi:10.1167/12.6.32

Introduction

Sensory systems in the brain must continually calibrate environmental variability in order to efficiently represent the world. One strategy for achieving this is adaptation, which may optimize energy consumption in the brain and improve estimates about what is happening around us (Clifford et al., 2007; Dahmen, Keating, Nodal, Schulz, & King, 2010; Kohn, 2007; Teich & Qian, 2003). Although commonly employed in psychophysical investigations of visual perception, sensory adaptation lacks a cogent functional explanation that unifies its neuronal and perceptual effects.

Two observations are common in psychophysical studies employing adaptation: impaired absolute sensitivity and improved relative sensitivity. After prolonged exposure to a single stimulus, subsequent stimuli appear shifted away from the adaptor. This "perceptual repulsion" is evident in the tilt, motion, and direction after-effects, as well as adaptation to higher-order constructs such as faces and biological motion (Gibson & Radner, 1937; Levinson & Sekuler, 1976; Troje, Sadr, Geyer, & Nakayama, 2006; Webster, Kaping, Mizokami, & Duhamel, 2004). Perceptual repulsion impairs absolute sensitivity, because it prevents a veridical representation of stimulus features (Bex, Bedingham, & Hammett, 1999; Clifford & Langley, 1996). However, impaired absolute sensitivity can be complemented by improved discrimination and detection (relative sensitivity), typically of stimuli within a limited range close to the adapting condition (Clifford & Langley, 1996; Clifford et al., 2001; Dahmen et al., 2010; Phinney, Bowd, & Patterson, 1997).

Most sensory neurons show a decrease in spiking activity when exposed to an ongoing stimulus. The magnitude of this adaptation depends on how closely the adapting stimulus matches the neuron's tuning and cannot be solely attributed to neurotransmitter depletion (Dragoi, Sharma, & Sur, 2000; Kohn & Movshon, 2004; Muller, Metha, Krauskopf, & Lennie, 1999). Adaptation can change the shape and gain of a neuron's tuning curve, commonly leading to a repulsive shift in the tuning curve peak away from the adaptor (Saul & Cynader, 1989a, 1989b). However, attractive tuning shifts have been reported in motion-sensitive neurons in the middle temporal area (Kohn & Movshon, 2004). Thus, the relationship between shifts in neuronal direction tuning curves and shifts in

doi: 10.1167/12.6.32 Received January 17, 2012; published June 22, 2012 ISSN 1534-7362

direction perception after adaptation remains to be clarified.

Computational models that decode the responses of populations of sensory neurons have given insights into how changes in absolute and relative perceptual sensitivity could arise from neuronal adaptation. However, they have been limited to adaptation protocols that incorporate exposure to long, monotonous stimulus conditions, rather than short-duration, widely distributed stimuli (Crowder et al., 2006; Dragoi et al., 2000; Kohn & Movshon, 2003; Petersen, Baker, & Allman, 1985). Therefore, it is unclear how either perceptual or neuronal adaptation is affected by rapid changes in motion over short durations.

We investigated how adaptation to stimuli comprising distributions of directions affects fine direction discrimination. Our psychophysical results and those of a neuronal decoding model confirm previous findings that the neurons best suited to supporting fine discrimination judgments have preferred directions 30–60° from the discrimination boundary. Surprisingly, compared with a uniform adaptation condition, stimuli designed to selectively adapt neurons preferring directions > 60° from a discrimination boundary significantly improved discrimination, whereas adapting stimuli comprising a distribution of directions ± 30–60° from the boundary impaired discrimination. Direction-specific changes in neuronal gain, which affect the population signal-to-noise ratio, are sufficient to account for changes in perceptual bias and threshold due to adaptation.

Methods

We developed a novel adaptation paradigm, in which the direction of a moving dot stimulus could be changed every 10 ms, allowing a distribution of motion directions to be developed over a 1500-ms adaptation period. By varying the relative probability with which a given direction was presented, we hypothesized that we could selectively adapt subpopulations of neurons with different preferred directions, allowing us to infer how direction perception depends on the activity of a population of neurons. In all tasks, subjects made fine discrimination judgments of linear motion direction relative to a vertical category boundary (e.g., left or right relative to vertical).

Subjects

Subjects were the two authors and seven volunteers from the Monash student and staff community who gave informed consent (two male; five female). All had normal or corrected-to-normal visual acuity. Four subjects were aware of the general aims of the study, but did not know the specific hypotheses. The remaining subjects were naïve with respect to the aims and hypotheses of the study. Not all subjects took part in all experiments.

Stimuli and task

Stimuli were generated using Matlab (The Mathworks, Natick, MA) and the Psychophysics Toolbox (Brainard, 1997; Pelli, 1997), and were viewed binocularly on a Sony Multiscan G500 monitor (1280 × 960 pixels; viewable area 400 × 300 mm; refresh rate 100 Hz; viewing distance 670 mm). To minimize eye movements, subjects used a chin- and forehead-rest and were asked to fixate a central red cross with sides 0.4° surrounded by a black circle of 0.8° diameter. Eye movements were not monitored.

Stimuli comprised 100 antialiased white dots of diameter 0.1° presented on a black background limited to a circular aperture of 5° diameter and centered around the fixation cross. Dots moved with speed 4°/s and were randomly replotted so as to maintain uniform dot density when they left the circular 5° aperture. Dot lifetime was 6 frames, with a total displacement for each dot of 0.2°.

The sequence within each trial was: adaptation period (1500 ms), blank screen (100 ms), and test period (150 ms). The motion direction during the adaptation period could be varied every 10 ms (see following). During the 150-ms test period, all dots moved in the same direction on every frame and always contained a component of upward motion. Test directions were presented using the method of constant stimuli with 6–12 repetitions of 7–9 directions presented in each block of trials. Subjects reported their perceived direction of the test motion relative to vertical with a key press (left or right). Reaction times were not monitored, and if subjects were uncertain of the direction on any trial, they were instructed to guess.

To aid perceptual judgments, the discrimination boundary was indicated throughout each trial as two vertical red lines extending from 0.5–2° beyond the edge of the dot aperture, aligned above and below the fixation cross. The presence of these lines did not significantly affect discrimination thresholds when the category boundary was vertical but was critical for some subjects when we tested with an oblique category boundary (data not shown). By convention, we will express adaptation and test directions relative to the category boundary, which was always vertically upward (0°). Judgments of "left" or "anticlockwise" were

given negative sign (< 0°); judgments of "right" or "clockwise" were positive (> 0°).

Adaptation direction distributions

During the adaptation period, the motion direction was either constant or varied randomly on every 10-ms frame according to predefined distributions. Our stimulus resembles a Motion Reverse Correlation stimulus employed previously (Borghuis et al., 2003; Perge et al., 2005), but allows us to independently define the probability of motion in each direction. When random distributions were used, all dots moved in the same direction on a single frame (i.e., 100% coherence) unless (1) they had reached the end of their 60-ms lifetime and were randomly replotted within the aperture or (2) they left the aperture and were replotted on the opposite side of the aperture to maintain uniform dot density. Dot directions were drawn from five different distributions and, except for the *Single* direction condition, were quantized to 12 possible directions in 30° steps:

(1) a *Single* direction condition (Figure 1A, 1D), of −30°, −15°, 0°, 15°, or 30°;
(2) a *Uniform* condition (Figure 1B, 1E) in which all 12 directions were presented with equal probability;
(3) an "*All Flanks*" condition in which only directions ± 30° and ± 60° relative to the category boundary were presented with equal (1/4) probability (Figure 1C, 1F);
(4) a complementary "*No Flanks*" condition in which all directions other than ± 30° and ± 60° relative to the category boundary were presented with equal (1/8) probability (Figure 1G)
(5) von Mises distributions with mean 0° and variable concentration parameter κ (Figure 1H, 1I).

Neurons in the middle temporal area (MT) are strongly implicated in direction perception (Britten et al., 1996; Newsome, Britten, & Movshon, 1989; Newsome & Pare, 1988; Price & Born, 2010; Salzman, Britten, & Newsome, 1990) and have direction tuning bandwidths of ~ 90° (Britten & Newsome, 1998; Price, Ibbotson, Ono, & Mustari, 2005). Thus, our nomenclature for the adaptation conditions reflects the fact that, for a neuron preferring upward motion, the *All Flanks* condition only presents motion on the tuning curve flanks. Conversely, the *No Flanks* condition never presents motion on the flanks of the tuning curve. A complementary way to consider this paradigm is that only neurons that have the category boundary on the flank of their tuning curve are strongly adapted by the *All Flanks* condition. The von Mises distributions with variable concentration around the 0° discrimination boundary were designed to test previous reports in the auditory system, showing that perceptual sensitivity close to a category boundary depends on the variance of an adapting stimulus distribution centered on that boundary (Dahmen et al., 2010). Four subjects were tested with κ values of 1.2, 4.2, and 100; three subjects were tested with $\kappa = 0.8$, 1, 1.6, 10, and 100. $\kappa = 0.8$, 1.6, and 10 produce distribution with 44%, 61%, and 98% of motion periods within ± 30° of the mean direction, respectively. $\kappa = 100$ is a single adaptation direction.

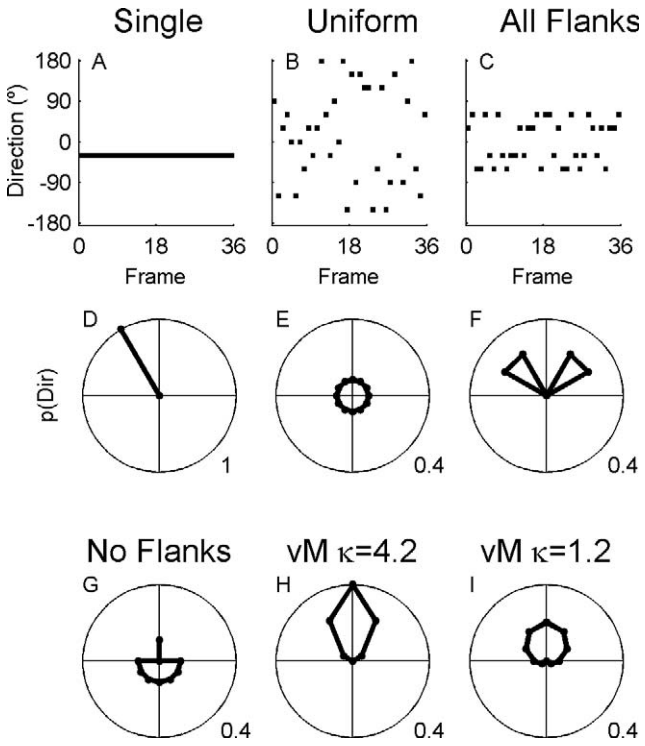

Figure 1. Stimulus direction sequences and probabilities. The standard adaptation protocol has a single, fixed direction throughout the adaptation period, shown here as 36 frames of direction −30° (A). Therefore, the probability of −30° is 1 and all other directions have probability 0. The probability distribution is shown in polar coordinates (B). Note that all directions are expressed relative to upward = 0° with positive directions clockwise. Single adaptation directions of 0°, ± 15°, and ± 30° were used. In the *Uniform* adaptation condition, all 12 directions have equal probability of presentation across time (B, E). In the *All Flanks* condition, only directions ± 30° and ± 60° relative to 0° are shown, with equal probability (C, F). The complementary distribution is the *No Flanks* condition (G). von Mises distributions (vM) centered on vertical 0° with variable concentration parameters were also employed (H–I); = 100 is a single direction due to the 30° quantization employed. = 1.2 and 4.2 are shown.

The adaptation conditions were either presented in blocks (i.e., all trials within a block of up to 96 trials had the same direction distribution) or interleaved (i.e., each trial within a block had a randomly chosen direction distribution). This allowed us to examine the

effects of any adaptation that accumulated over a ~ 5 minute block of trials.

Analysis

For each adaptation condition, each subject ran at least 56 trials (eight repetitions of seven test directions); however, on average, 155 trials were completed for each adaptation condition. Data is presented as the percentage of trials in which a subject reported the test direction as "right" or "clockwise" with respect to the 0° vertical category boundary. Logistic curves (Equation 1) were fit to the raw data using maximum likelihood methods,

$$p_{right}(\theta) = \gamma + (1 - \gamma - \lambda)\frac{100}{1 + \exp\left(-(\theta - \alpha)/\beta\right)}, \quad (1)$$

where $p_{right}(\theta)$ is the percentage of trials with test direction θ reported "right" of the category boundary; α is the point of subjective equality (PSE); β is the slope, which is equivalent to the threshold e / (1+e) or 73.1% correct; and γ and λ are the lower and upper plateaus.

In practice, the four-parameter logistic curve was rarely better than a two-parameter fit in which we constrained $\gamma = \lambda = 0$ (F-test and likelihood ratio test, $p > 0.05$), thus for simplicity we only refer to PSEs and thresholds obtained from two parameter fits.

A bootstrap method, which fit 199 subsampled data sets for each adaptation condition, was used to determine standard errors on fit parameters. To compare the effects of two or more adaptation conditions on a single subject, we applied a two-sample t-test or ANOVA to the distributions of PSEs or thresholds obtained from the bootstrapped fits to the data.

Results

Perceptual repulsion

A common effect of prolonged adaptation to a single-motion direction is perceptual repulsion, referred to as the direction aftereffect (Levinson & Sekuler, 1976; Schrater & Simoncelli, 1998). We replicated this observation using adaptation durations of 1,500 ms, presented in both blocked and interleaved conditions. In our initial testing with blocked conditions, all adaptation stimuli within a block of 56–96 trials had the same direction of either 0°, +15°, or −15° relative to upward. In the interleaved condition, the adaptation direction for each trial was randomly chosen from 0°, +30°, or −30°, preventing any cumulative effects of adaptation across trials. The adaptation directions used in the interleaved conditions conform to the 30° quantization used in the dynamic adaptation experiments described later. Figure 2A shows the results from a single observer tested with the blocked design. After adaptation to motion 15° left of vertical, the subject is biased to report subsequent test directions as moving rightward. Conversely, after adaptation to the right, perceptual reports are biased to the left. Note that the phenomenon of perceptual repulsion is characterized by shifts of the psychometric curve toward the adapting condition.

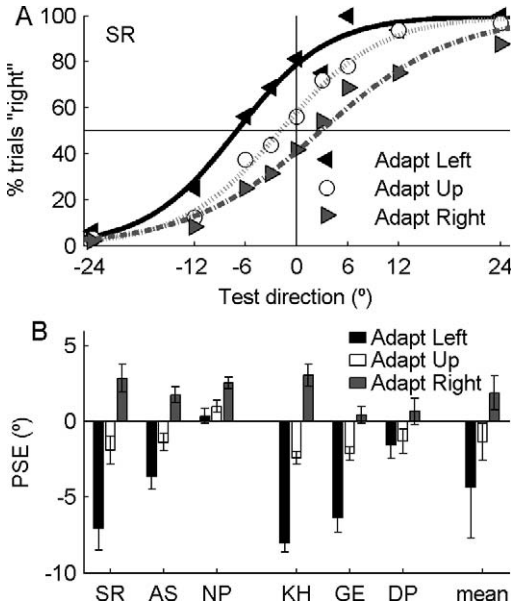

Figure 2. Perceptual repulsion after adaptation to a single direction. (A) Psychophysical curves for a single subject after adaptation to 1,500 ms of motion −15°, 0°, and 15° relative to vertically upward (0°). Adaptation conditions were presented in blocks. (B) Summary of performance for six subjects and averaged across all subjects. The point of subjective equality (PSE) was obtained from logistic curves fit to the raw data. Error bars show standard deviation of the bootstrapped fit parameters for individual subjects and standard deviation across subjects for the mean. Adaptation conditions were presented in Blocks (SR, AS, NP) or Interleaved (KH, GE, DP).

A logistic curve was fit to each set of raw data using maximum likelihood fitting methods. The point of subjective equality (PSE) is the test direction at which 50% of trials are reported as both right and left of the vertical category boundary. PSEs are shown for three adaptation directions for six subjects, together with the mean across subjects (Figure 2B). In each case, PSEs associated with adaptation to leftward motion are more negative than PSEs associated with adaptation to upward motion, which are in turn more negative than PSEs associated with adaptation to rightward motion. Based on an ANOVA applied to the distribution of

PSEs from 199 bootstrapped fits to the raw data, these PSE differences are significant for all subjects except DP ($p < 0.01$). For subject DP, while there was no significant difference between Adapt Left and Adapt Up, the Adapt Right condition was significantly greater ($p < 0.01$) than both the Adapt Left and Adapt Up conditions. The trends across all subjects demonstrate that a clear direction aftereffect can be produced by 1,500 ms of adaptation, even when trials with different adaptation directions are interleaved.

Selective adaptation can improve and impair discrimination

We found that selective exposure to different distributions of adaptation directions could both improve and impair discrimination performance relative to a control condition in which all directions were presented. Figure 3A shows the discrimination performance of two subjects after adaptation to the *All Flanks* and *No Flanks* conditions. The *All Flanks* condition only presents motion in directions ± 30° or ± 60° relative to the upward category boundary, whereas the *No Flanks* condition never presents motion in these directions. Both subjects were more sensitive after exposure to the *No Flanks* condition (▼) than the *All Flanks* condition (Δ) as evidenced by the increase in slope and decrease in threshold (Figure 3A).

With blocked adaptation, the *Uniform* condition typically produced thresholds that were intermediate between those of the *No Flanks* and *All Flanks* conditions (Figure 3B). These data points fall into the lower-right quadrant of Figure 3D, which compares threshold ratios for *No Flanks* and *All Flanks* with the control *Uniform* condition. This trend was significant ($p < 0.01$, one-way ANOVA) in all subjects except AS and DP. In all subjects, the thresholds for the *All Flanks* condition were significantly higher than those for the *No Flanks* condition ($p < 0.01$). An unresolved question in the literature has been whether different adaptation conditions under the same protocol can enhance or only impair perceptual sensitivity. Our results suggest that, relative to "baseline" adaptation to a uniform distribution of directions, judicious choice of a distribution of adaptation directions can either impair or improve direction discrimination.

Although the adaptation duration in individual trials was only 1,500 ms, we were concerned that the effects of this adaptation could accumulate across multiple identical trials. To address this, we repeated the same protocol, but with the three adaptation conditions randomly interleaved. Because the motion directions in the *All Flanks* and *No Flanks* conditions are complementary, across a block of trials, subjects have near-uniform exposure to all adaptation directions. Note

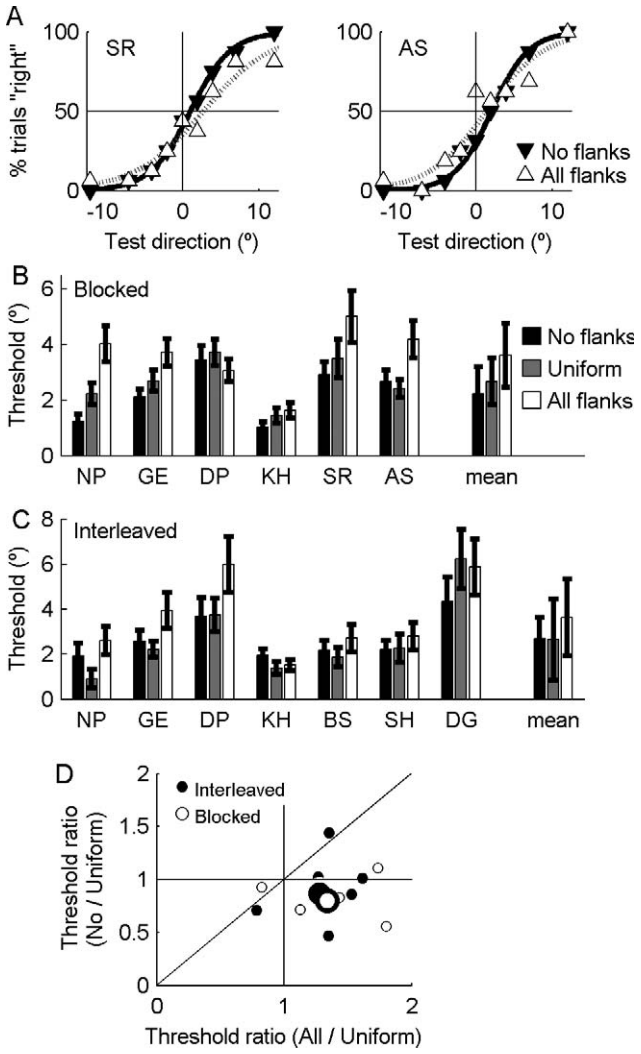

Figure 3. Changes in perceptual sensitivity associated with *No Flanks*, *All Flanks,* and *Uniform* adaptation distributions. (A) Psychophysical performance of two subjects after adaptation to *No Flanks* and *All Flanks* conditions presented in blocked conditions. Psychophysical thresholds obtained from logistic curves fit to the raw data are shown for subjects tested with blocked (B) and interleaved (C) adaptation conditions. Steeper psychometric curves correspond to higher perceptual sensitivity and lower thresholds. Mean thresholds across all subjects are shown on the right of each plot. Error bars show standard deviations of the bootstrapped fit parameters for individual subjects and standard deviation across subjects for the mean. (D) Threshold ratios obtained in the *No Flanks* and *Uniform* adaptation conditions compared with the threshold ratios obtained in the *All Flanks* and *Uniform* conditions. Small circles are data for individual subjects; large circles are the geometric mean across subjects. Values below the line of unity indicate greater sensitivity following *No Flanks* than *All Flanks*. Values in the lower right quadrant indicate a progression of sensitivity from *No Flanks,* to *Uniform,* to *All Flanks* conditions.

that across the entire testing protocol there is a small over-representation of directions with an upward component because of the test conditions and a small over-representation of ± 30 and ± 60° because there are fewer directions in the *All Flanks* condition than the *No Flanks* condition. Despite this, thresholds associated with the *No Flanks* condition were equal to or lower than thresholds in the *All Flanks* condition (Figure 3C) and fall below the line of unity in the comparison of threshold ratios (Figure 3D). These differences were significant in six of seven subjects ($p < 0.01$). The only subject for whom this trend was not observed (DG) expressed difficulty in understanding the task and had the highest thresholds.

Direction range does not affect discrimination performance

Previous reports have shown that perceptual sensitivity close to a category boundary scales with the range, or variance, of an adapting stimulus distribution centered on that boundary (Dahmen et al., 2010). In our experiments, this suggests that direction discrimination thresholds should increase as the range of adaptation directions centered on 0° is increased. However, the choice of an upward-centered adapting distribution may have little effect on performance, as our earlier experiments demonstrated that it is primarily adaptation to directions ± 30–60° from the discrimination boundary that affects discrimination. We tested this by varying "κ," the concentration parameter of a von Mises distribution, with a mean upward direction. Figure 4A shows perceptual thresholds for seven subjects tested after adaptation to different direction ranges. The same data is shown in Figure 4B, normalized relative to the threshold obtained with a uniform distribution of directions. Across subjects, there are no systematic changes in threshold with direction range, even when the adaptation conditions were blocked (data not shown). This suggests that, in this paradigm, discrimination thresholds do not depend on the variance of directions around the discrimination boundary.

A stochastic population decoding model

Previous computational models of motion adaptation have attempted to explain the effects of sustained exposure to a single stimulus feature on neuronal and perceptual sensitivity (Gilbert & Wiesel, 1990; Kohn & Movshon, 2004; Teich & Qian, 2003). Here, we develop a neuronal population decoding model that accounts for both perceptual repulsion induced by adaptation to a single direction (Figure 2) and our observed changes

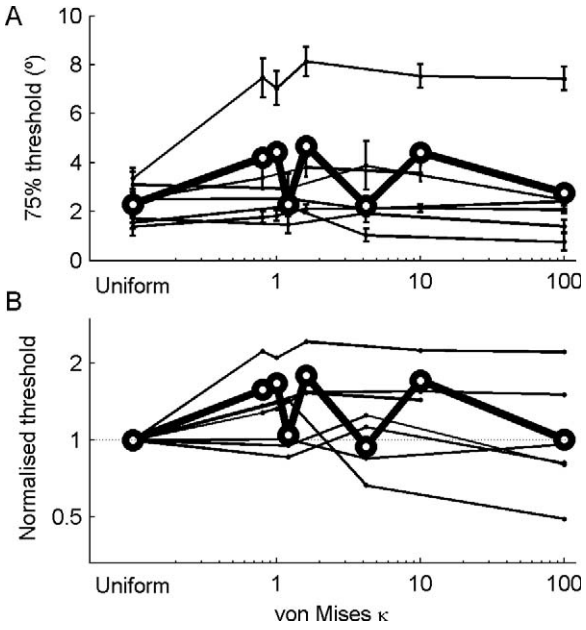

Figure 4. Effect of adaptation direction range on perceptual threshold. Raw (A) and Normalized (B) perceptual thresholds for seven subjects. Thresholds for individual subjects are shown as thin black lines. The thick line is the mean across subjects (geometric mean in B). von Mises κ controls the concentration of the direction distribution; small values lead to a uniform probability of all directions being presented; high values lead to only a single direction being presented. Error bars in A show standard deviation of the bootstrapped fit parameters.

in perceptual threshold following adaptation to distributions of directions (Figure 3). This requires a model that incorporates the stochastic nature of neuronal responses, as this variability affects perceptual thresholds. Postadaptation changes in perceptual performance could be attributed to changes in neuronal gain (i.e., the mean firing rate), tuning curve shape, intertrial response variability, interneuronal correlation structure, or the synaptic weights of feed-forward connections, but psychophysical and modeling data cannot address which of these physiological mechanisms might be most important. Thus we begin by examining the effect of changes in neuronal gain, which are the simplest and most robust consequence of adaptation. Subsequently, we examine the effects of changes in tuning curve shape by varying each neuron's preferred direction without any change in neuronal gain. Thus, two major effects of adaptation are investigated separately: changes in gain and changes in preferred direction.

The model incorporates a population of 72 MT-like, direction-selective neurons, with preferred directions uniformly separated by 5°. Each neuron had a mean direction tuning response defined by a von Mises function, which closely approximates the tuning curves of most MT neurons (Figure 5A):

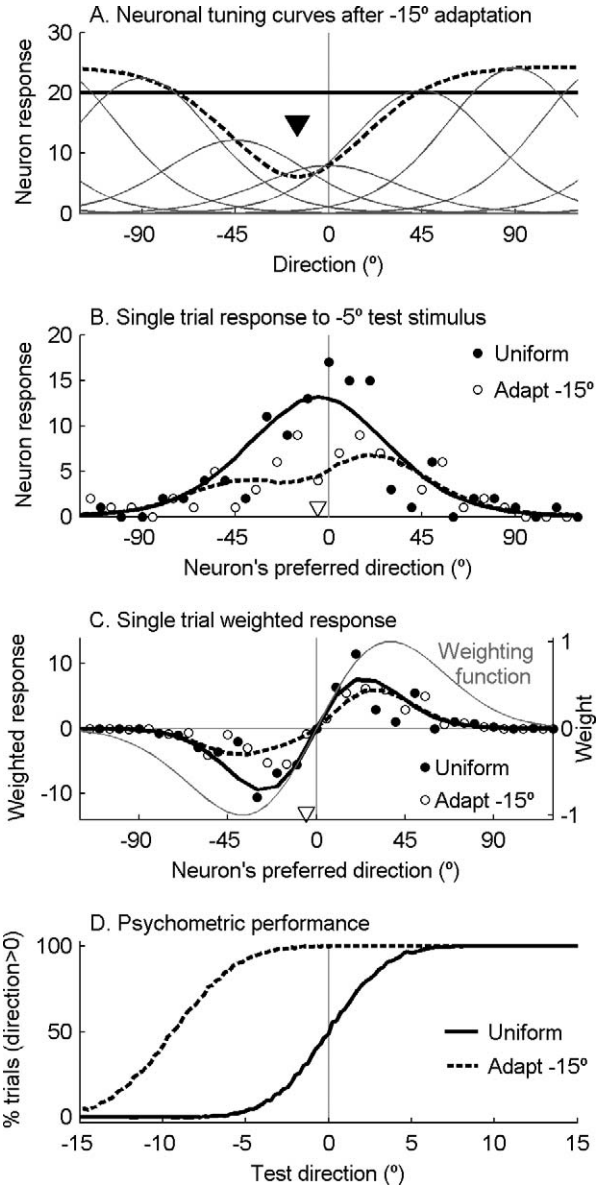

Figure 5. Processing steps within the neuronal population decoding model. (A) Direction tuning curves (thin solid lines) of representative neurons with preferred directions separated by 45°, after adaptation to −15° (▼). The mean response of each neuron at its preferred direction is indicated by the gain envelope for uniform adaptation (solid line) and after adaptation to −15° (dashed line). (B) Responses of the adapted (°) and unadapted (•) neuronal population to a single trial of a −5° test stimulus (▽). (C) Weighted responses for the adapted and unadapted neuronal population for the same −5° test trial shown in B. Thick lines in B and C show the mean response across 2,000 simulated trials. (D) Psychometric performance, quantified as the percentage of trials in which the summed weighted response is greater than 0.

$$\overline{R_i(\theta)} = g.g_{i,adapt}.\exp\Big(\kappa.\cos(\theta - \theta_{i,pref})\Big). \quad (2)$$

$\overline{R_i(\theta)}$ is the mean response of neuron i, with preferred direction $\theta_{i,pref}$, to test direction θ; the von Mises concentration factor κ was set to 3 for all neurons, giving a tuning bandwidth of 77°; g controls the global response gain or maximum firing rate across all neurons; and $g_{i,adapt}$ controls the scaling of responses due to adaptation, and is set to 1 in the absence of adaptation (see following).

To mimic the stochastic nature of normal neuronal activity, single-trial responses of each modeled neuron were randomly drawn from a Poisson distribution with mean set by Equation 2. Importantly, the only parameters in the model that are changed across all simulations shown here are the gains for each neuron (g, $g_{i,adapt}$), which were systematically changed to represent different adaptation conditions. The reduction in each neuron's gain is proportional to the prevalence of that neuron's preferred direction in the adapting distribution.

The effects of adaptation to a single direction (e.g., −15° indicated by the arrowhead in Figure 5A) are summarized by the gain envelope ($g_{i,adapt}$) implemented by scaling an inverted von Mises function so that the response suppression produced by a given stimulus is proportional to the separation of the adaptation and preferred directions (Equation 3, dashed line in Figure 5A). Setting $\kappa_{\text{adapt}} = 3$ ensured that neuronal gain is minimally affected by stimuli greater than 60° from a neuron's preferred direction (Kohn & Movshon, 2004; Yang & Lisberger, 2009).

$$g_{adapt}(\theta_{pref}) = 1 - d\frac{\exp\Big(\kappa_{adapt}.\cos(\theta_{pref} - \theta_{adapt})\Big) - \exp(-\kappa_{adapt})}{\exp(\kappa_{adapt}) - \exp(-\kappa_{adapt})} \quad (3)$$

g_{adapt} is the scale factor applied to the response of a neuron with preferred direction θ_{pref} after adaptation to direction θ_{adapt}. d controls the maximum response suppression, or depth of adaptation by limiting g_{adapt} to the range $(1 - d, 1)$. We set $d = 0.75$.

There is no existing physiological data that guides how to model the effects of adaptation to a distribution of directions, thus the effects of adaptation to each direction in an adapting distribution were linearly combined (Equation 4),

$$g_{adapt}(\theta_{pref}) = 1 - \frac{d}{n_j}.$$

$$\sum_j \frac{\exp\Big(\kappa_{adapt}.\cos(\theta_{pref} - \theta_{adapt,j})\Big) - \exp(-\kappa_{adapt})}{\exp(\kappa_{adapt}) - \exp(-\kappa_{adapt})}, \quad (4)$$

where there are n_j unique adaptation directions $\theta_{adapt,j}$

Figure 5B shows the single trial responses of 36 simulated neurons to a −5° test direction in an unadapted state (•) and after adaptation to −15° (°). The solid lines show the mean response across 2,000

trials. To generate a discrimination judgment for a single trial of a given stimulus, a population response R_{pop} was calculated from the weighted sum of the responses of all neurons (Equation 5, Figure 5C). The judgment on each trial is determined by the sign of R_{pop}: $R_{pop} > 0$ votes for positive directions (i.e., right relative to the category boundary) whereas $R_{pop} < 0$ votes negative or left. A Gabor function with $\sigma = 1$ (Equation 5, Figure 5C) was chosen as the weighting function so that neurons with preferred directions of ±30–45° relative to the discrimination boundary contribute most strongly to the judgment.

$$R_{pop}(\theta) = \sum_i R_i(\theta).\exp\left(-\left(\frac{\theta_{i,pref}}{\sigma}\right)^2\right).\sin(\theta_{i,pref}) \quad (5)$$

For the single trial simulated in Figure 5B and C, $R_{pop}(\theta = -5°) > 0$ after adaptation, but $R_{pop}(\theta = -5°) < 0$ in the unadapted, uniform condition. Thus, for these trials, the perceptual judgment is "right" after adaptation to −15°, but "left" when there was no adaptation. Because discrimination performance can only be quantified after the responses to many repeated trials, we examined the outputs of the model to 2,000 repetitions of test directions between −15° and 15° in 0.25° steps. Figure 5D summarizes the data in the same format as the human psychophysical performance, allowing quantification of performance using the same metrics, PSE and threshold. Perceptual repulsion is clearly evident in the example adaptation to −15°; adaptation to a stimulus slightly left of the category boundary selectively reduces the gain of neurons with preferred neurons similar to the adaptor, biasing the model to report subsequent motion as right of the category boundary. In summary, perceptual repulsion is associated with PSEs shifting toward the adaptation condition.

Gain changes alone can account for the diverse effects of adaptation

The model's discrimination performance increases as both the number of neurons (data not shown) and the average gain are increased (Figure 6A–6C). This is simply because, in both cases, more independent information (i.e., more spikes) is available to encode the stimulus. However, we are primarily interested in how model performance is affected by differences in gain between neurons that prefer different directions; i.e., it is *relative* gain across the population that is under investigation here, not *absolute* gain. Therefore, to compare the effects of relative gain in different instantiations of the model, we used a fixed population of 72 neurons and normalized responses by setting average gain across the population to 20 (Equation 6). This gives a baseline sensitivity similar to human perceptual discrimination performance (Figure 6B). Note that the only free parameters in the model are the gains of the individual neurons. All other parameters (e.g., number of neurons, direction tuning bandwidth, preferred direction, weighting function, Poisson variability) are fixed and the same in every iteration of the model. The result of the gain normalization is that the mean firing rate of some neurons must be scaled up to compensate for adaptation-induced reductions in the gain of other neurons (e.g., Figure 6D). While this increase might seem surprising (Kohn & Movshon, 2004; Van Wezel & Britten, 2002), it is a feature of divisive normalization models (Simoncelli & Heeger, 1998) and has been reported in MT neurons (Petersen et al., 1985).

$$g = \frac{20}{\sum_i g_{i,adapt}} \quad (6)$$

Figure 6D shows neuronal gains across the population after adaptation to −30°, 0°, or 30°, with the corresponding psychometric functions shown in Figure 6E. Reducing the gain of neurons with preferred directions close to an adaptation direction produced shifts of the modeled psychometric function consistent with perceptual repulsion. We investigated the effects of adaptation to single directions from −90° to 90° in 5° steps. While the largest changes in the point of subjective equality (PSE) were for adaptation directions of ± 30° (Figure 6F), this "optimum" adaptation direction depends on a neuron's tuning bandwidth and the weighting function (Equation 5), which governs how much each neuron contributes to the judgment. Importantly, perceptual repulsion was reproduced in the model regardless of the width of the dip in the gain envelope (κ_{adapt}), how strongly the gain was reduced at the adaptation direction (d) or σ in the weighting function (data not shown).

The model also reproduces the relative changes in perceptual sensitivity associated with the *All Flanks* and *No Flanks* adaptation conditions (Figure 6G–6I). Figure 6G shows the neuronal gains after adaptation equivalent to the *All Flanks, No Flanks* and *Uniform* conditions used in the psychophysical testing. As the gain envelopes are symmetrical about the 0° category boundary, there is no lateral shift in the psychometric function, and PSE = 0 in each case. However, there are clear changes in threshold; as observed in the human data, performance is best after adaptation to the *No Flanks* condition and worst after the *All Flanks* condition (Figure 6H).

In general, the *All Flanks* condition is defined by the presence of two adaptation directions symmetric about the discrimination boundary (e.g., +45° and −45°), whereas the *No Flanks* condition is defined by the presence of all complementary adaptation directions

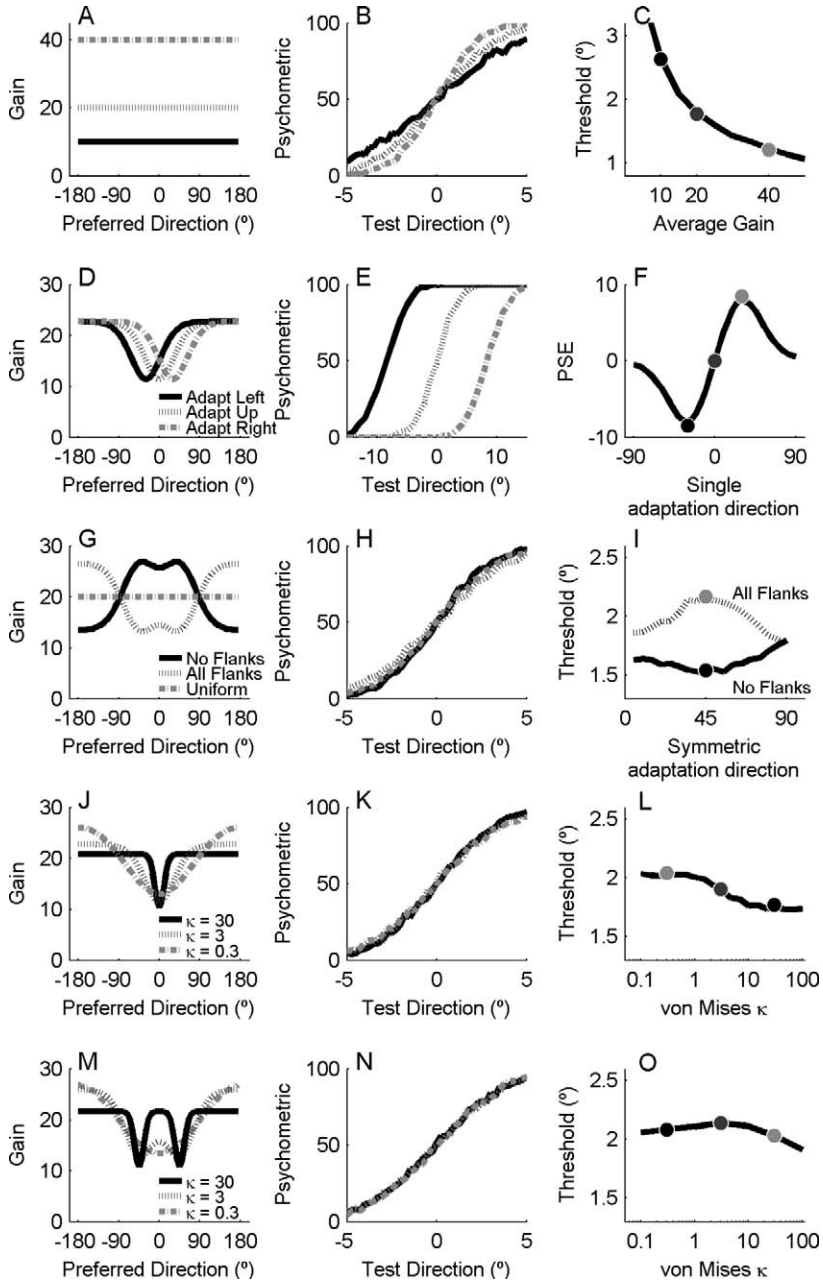

Figure 6. Model outputs with gain envelopes (g, g_{adapt}) produced by different adaptation conditions (A–C: changes in average gain; D–F: single direction; G–I: *All Flanks* or *No Flanks*; J–L: range of directions centered on 0°; M–O: range of directions for *All Flanks* centered on ± 45°). The middle column (B, E, H, K) shows the psychometric performance associated with three gain envelopes in the left column (A, D, G, J). Model performance across a range of gain envelopes is shown in the right column with solid markers indicating the corresponding PSE (C) or threshold (F, I, L, O) for the three sample gain envelopes shown in the left column.

(Figure 1F, 1G). To systematically examine the role of these symmetric adaptors, we determined psychometric thresholds for *All* and *No Flanks* adaptation conditions based on symmetric directions ranging from ± 5° to ± 90° in 5° steps (Figure 6I). *No Flanks* adaptation always enhanced performance relative to the *All Flanks* condition, with the separation maximized when directions ± 45° were only, or never, adapted.

In the human psychophysical data, varying the range of adaptation directions around the 0° category boundary had little effect on discrimination performance. A similar effect was observed when we varied the bandwidth of the postadaptation gain envelope in the model by varying the von Mises concentration parameter κ_{adapt}. The neuronal gains (Figure 6J) and corresponding psychometric curves (Figure 6K) for

three direction ranges are shown with performance varying only slightly across conditions. With a broader ranger of concentrations (Figure 6L), threshold decreases only marginally as the range of adaptation is decreased (increasing κ_{adapt}). This is because, regardless of the adaptation range, the neurons with the largest changes in gain are those with preferred directions of 0°, which do not greatly contribute to the summed population response because of the response weighting function (Equation 5).

We also examined how a range of symmetric adaptation directions centered on ± 45° affected model performance (Figure 6M,N). Varying κ from 0.1 to 100 produced little change in threshold (Figure 6O), primarily because the gain of the informative neurons with preferred directions of ± 45° was substantially reduced in all conditions.

Attractive shifts in direction tuning can account for perceptual adaptation

Having demonstrated that changes in gain are sufficient to reproduce the perceptual effects of adaptation, we now investigate whether lateral shifts in a neuron's direction tuning curve, with no changes in gain or bandwidth, can also account for perceptual adaptation. For each neuron, the stimulus directions that evoke the largest mean firing rates before and after adaptation are referred to as the pre- and postadaptation preferred directions, respectively ($\theta_{pref,pre}$ and $\theta_{pref,post}$). The magnitude of the shift in each neuron's direction tuning curve depended on the separation between the neuron's preferred direction and the adaptation direction (Equation 7),

$$\begin{aligned}\theta_{shift} &= \theta_{pref,post} - \theta_{pref,pre} \\ &= S.\left(f(\theta_{pref,pre}, \theta_{adapt})\right).\exp\left(\frac{f(\theta_{pref,pre}, \theta_{adapt})}{-\sigma_{shift}}\right)^2,\end{aligned} \quad (7)$$

where $f(\theta_{pref,pre}, \theta_{adapt})$ was simply $\theta_{pref,pre} - \theta_{adapt}$, but was shifted by 360° as appropriate to be in the range (−180, 180).

σ_{shift} and S control the range of neurons that experience direction shifts and the size of the shifts, respectively. To match previously observed physiological shifts in direction tuning in area MT, we set $\sigma_{shift} =$ 45° (Kohn & Movshon, 2004). S was systematically varied to adjust the size of the peak shift: $S > 0$ produces repulsive shifts, moving direction tuning curves away from the adapting condition; conversely, $S < 0$ produces attractive shifts, moving a neuron's preferred direction towards the adapting condition (Figure 7A,B). We limited $|S| < 1$, so that, with the strongest attractive shifts, a neuron's postadaptation preferred direction could never shift enough to match the adaptation direction. The effects of simultaneous adaptation to multiple directions were assumed to be independent, so the shifts associated with each adaptation direction were summed.

The pattern of shifts in preferred direction across the population of neurons is shown for $\theta_{adapt} = 0°$ with $S =$ −0.8, 0, and 0.8 (Figure 7B). Relative to the condition in which no shifts in preferred direction occur ($S = 0$), thresholds were increased by attractive shifts and slightly decreased by repulsive shifts (Figure 7C). These changes in threshold are accompanied by changes in PSE when adaptation occurs at directions not aligned with the discrimination boundary. The changes in preferred direction after adaptation to −30°, 0°, and 30° are shown for $S = -0.8$ and +0.8 (Figure 7D and 7F), with the corresponding PSEs shown as circles in Figure 7E and 7G. Notably, attractive shifts in neuronal tuning consistently produce changes in PSE that would predict perceptual repulsion (Figure 7E) as was observed psychophysically. With $S > 0$ so that adaptation produces repulsive shifts in preferred direction, the changes in model PSE are the opposite of those reported perceptually (compare Figures 2B, 6F, and 7G).

Finally, we investigated the effects of simultaneous adaptation to multiple directions (*All Flanks* and *No Flanks*), which produce complex patterns of shifts in preferred direction because the effects of each adaptation direction are summed (Figure 7H). With adaptation centered at ± 45° and $S = -0.4$ to give attractive shifts in neuronal tuning, there is odd-symmetry about 0° in the pattern of direction shifts, leading to no change in PSE. A complicated dependence of threshold on adaptation direction emerges (Figure 7I), which is not reflected in our perceptual data nor observed in the model that only incorporates adaptation-induced gain changes.

Discussion

We have demonstrated three primary results. First, changes in perceptual performance can be induced by short exposure to stimuli with dynamically changing directions. Second, adaptation to different direction distributions can impair or enhance discrimination performance relative to a baseline uniform adaptation condition. Finally, our observed changes in psychophysical PSE and threshold are captured by a neuronal population decoding model in which adaptation changes neuronal gain. In the following, we discuss the timescales of adaptation, which neurons are likely to be informative for fine discrimination judgments,

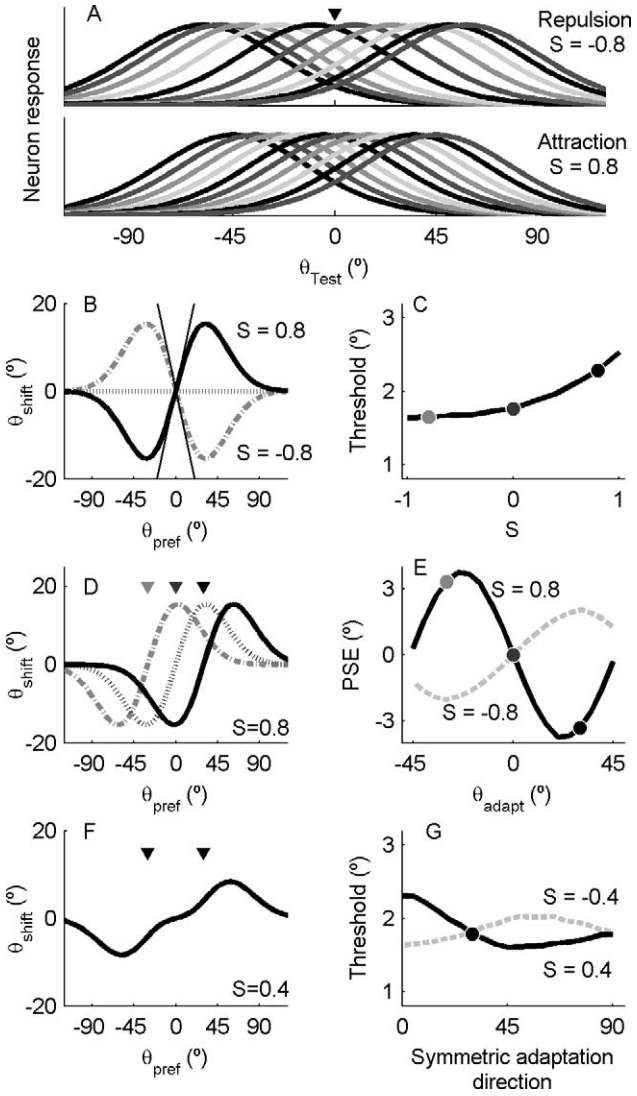

Figure 7. Model outputs associated with lateral shifts in direction tuning curves. (A) Attractive ($S = -0.8$) and repulsive ($S = +0.8$) shifts in direction tuning curves after adaptation to 0°, for 10 neurons with preadaptation preferred directions of −45° to 45° in 10° steps. (B) Shifts in the peak of the direction tuning curve, as a function of a neuron's preadaptation preferred direction, for model parameters $\theta_{adapt} = 0°$ and $S = -0.8$, 0, or 0.8. (C) Compared with the no adaptation case ($S = 0$), attractive direction tuning shifts ($S < 0$) increase discrimination thresholds, whereas repulsive shifts ($S > 0$) marginally reduce thresholds and therefore improve discrimination performance. Shifts in tuning curves after adaptation to −30°, 0°, and 30°, are shown for $S = 0.8$ (D). Arrowheads mark the adapting direction. The corresponding PSEs are shown as the colored circles in panel E. For adaptation directions > 30° from the discrimination boundary, attractive shifts in tuning curves produce repulsive shifts in perceived direction, whereas repulsive shifts in tuning curve lead to attractive shifts in perceived direction (E). A linear combination of attractive shifts associated with the *No Flanks* or *All Flanks* adaptation conditions produces complex shifts in preferred direction (*F*, $S = 0.4$, $\theta_{adapt} = \pm 30°$). The changes in threshold for a range of symmetric *No Flanks* and *All Flanks* adaptation conditions are shown in G.

and the scenarios in which adaptation to stimulus statistics may not be evident.

Selective adaptation of the informative neurons

A wealth of evidence suggests that motion perception and direction discrimination are dependent on neuronal activity in cortical area MT (Britten et al., 1996; Newsome et al., 1989; Newsome & Pare, 1988; Salzman et al., 1990). From both psychophysical studies (Hol & Treue, 2001; Raymond, 1993; Sheth, Ventura, & Wu, 2009; Treue, Hol, & Rauber, 2000) and computational modeling (Graf, Kohn, Jazayeri, & Movshon, 2011), it has been suggested that the most informative neurons for fine direction discrimination are those with preferred directions 30–60° away from the discrimination boundary. Intuitively, this can be explained by the observation that, for most MT neurons, the portion of the tuning curve 30–60° away from the preferred direction has the steepest slope. The *All Flanks* and *No Flanks* adaptation protocols were designed to exploit these observations. Our psychophysical and modeling results are in accordance with previous findings; however, we now show that perceptual adaptation can be achieved on timescales of hundreds of milliseconds using stimuli with dynamically varying directions, in which successive frames have low probabilities of being in the same direction.

Our modeling is aligned with previous studies demonstrating that adaptation-induced attractive shifts in neuronal tuning curves could account for perceptual repulsion from the adapting stimulus (Gilbert & Wiesel, 1990; Jin, Dragoi, Sur, & Seung, 2005; Kohn & Movshon, 2004). However, V1 neurons typically show no shifts or repulsive shifts in tuning curve following adaptation (Felsen et al., 2002). While physiological studies of adaptation in MT neurons have observed attractive tuning curve shifts when grating stimuli are employed, no systematic shifts in direction tuning are observed for stimuli comprising random dot patterns (Kohn & Movshon, 2004; Yang & Lisberger, 2009). Importantly, in both V1 and MT, adaptation produces reliable changes in response gain. It remains to be explained why the direction-specific effects of adaptation in MT should depend on the spatial structure of the adapting stimulus, but our modeling results suggest these tuning shifts may be of secondary importance.

Perceptual repulsion, as well as changes in perception associated with simultaneous adaptation to multiple directions (the *All Flanks* and *No Flanks* conditions) are completely accounted for by a model in which adaptation changes neuronal gain. Given that adaptation to dot stimuli produce little change in the

preferred direction of MT neurons, but still produce perceptual repulsion, it is likely that the perceptual effects described here are primarily related to changes in neuronal gain. Further, while neuronal gain changes and direction shifts could occur in conjunction (Jin et al., 2005), a primary role of neuronal gain changes in accounting for perceptual adaptation is supported by the reliable observation of decreases in neuronal gain for neurons with preferred directions similar to the adaptor.

The different adaptation conditions allowed us to rapidly vary motion direction while ensuring that we systematically presented a known stimulus distribution over the adaptation period. This approach is fundamentally different to two existing techniques for presenting multiple motion directions; both plaids and transparent motion use multiple, spatially overlapping stimuli with fixed directions maintained over time (Movshon, Adelson, Gizzi, & Newsome, 1985; Snowden, Treue, Erickson, & Andersen, 1991; Treue et al., 2000). Plaids have a practical drawback in that it becomes difficult to simultaneously present more than two directions, and further, the concurrent presentation of orthogonal orientations or motion directions in the same region of space can lead to cross-orientation suppression (Bonds, 1989; Morrone, Burr, & Maffei, 1982). Many studies have used random dot stimuli in which individual dot directions on each frame are drawn from a distribution of possible directions (Watamaniuk, Sekuler, & Williams, 1989; Williams & Sekuler, 1984). In these stimuli, the local motion direction varies across space in each frame, and the typical percept with a biased distribution of directions is motion in the mean direction of the distribution. When direction distributions are bimodal or multimodal, a global coherent motion percept is less common and eventually breaks down into transparent motion (Williams & Sekuler, 1984). In the context of adaptation, a stimulus with spatially interleaved directions would have the advantage that it maintains uniform energy in all directions over time, but the energy in each direction is reduced. Significantly, because such stimuli often lead to a global coherent percept, it is unclear how such a stimulus will adapt local motion sensitive neurons. For example, will perceptual adaptation be affected by the single perceived direction or the range of local motion directions?

In contrast, our approach has all visible dots move in the same direction, maximizing motion energy on each frame, but this direction is varied across time. The perception is of a single surface that rapidly changes direction or appears to jitter randomly. Our approach has the advantage that relative exposure to many different directions can be precisely controlled, and we can avoid effects such as cross-orientation suppression. However, this has the significant disadvantage that adaptation effects are nonuniform over time,with the most recent frames of the adapting stimulus likely to have the strongest effect on subsequent perception. While the temporally interleaved approach allows the application of reverse correlation techniques (Iyer, Freeman, McDonald, & Clifford, 2011), we had insufficient trials to attempt such an analysis here. Importantly, when integrated over space and time, the spatially and temporally interleaved approaches can contain equal numbers of dot-displacements in each direction in a desired distribution. Despite this, they are likely to have different effects at the neuronal and perceptual level because motion information is not integrated uniformly over space and time.

Rapid adaptation and limitations of the model

Previous studies of perceptual adaptation have commonly used single-adaptation stimuli presented for durations of many seconds. Our study is unique in that we could change the stimulus direction every 10 ms (1 monitor frame) and used a total adaptation duration of 1,500 ms. Neurons in MT can encode such rapidly changing stimuli, but their responses represent a time-weighted average of recent stimuli (Bair & Movshon, 2004; Borghuis et al., 2003; Buracas, Zador, DeWeese, & Albright, 1998; Perge et al., 2005; Priebe & Lisberger, 2002). Despite the short adaptation durations and range of stimulus directions, we observed robust perceptual repulsion following adaptation to a single direction that is consistent with previous studies using longer adaptation directions (Curran, Clifford, & Benton, 2006; Levinson & Sekuler, 1976; Wenderoth & Wiese, 2008). Recently, it has been shown that as little as two frames of motion can bias subsequent motion perception with the effects of just 67 ms of adaptation lasting for up to 1 second (Glasser, Tsui, Pack, & Tadin, 2011), thus it is reasonable to assume that adaptation produced by the individual motion steps in our stimulus accumulates throughout the adaptation period.

A novel finding was that, in comparison with the *Uniform* adaptation condition in which all motion directions were equiprobable, sensitivity was impaired following adaptation to the *All Flanks* distribution and enhanced following the *No Flanks* condition. Surprisingly, performance changes occurred even though, within a trial, the total duration of motion in any direction was very short. For example, in the *No Flanks* condition, eight directions were used, so on average, there were only 18.75 frames of motion in each direction, and only a one in eight probability of consecutive frames having the same direction. While it is unclear how the adaptation effects might accumu-

late over time, the effects of adaptation over different timescales could be incorporated into our model simply by increasing any changes in relative gain across the population. However, it is not clear how this may also affect absolute gain across the population, which has a more profound effect on discrimination performance in the model.

In the visual cortex, the timescales of neuronal adaptation span orders of magnitude, with time constants for the changes in firing rate produced by *unchanging* stimuli ranging from tens of milliseconds (Priebe, Churchland, & Lisberger, 2002; Priebe & Lisberger, 2002) through to tens of seconds (Dragoi et al., 2000). In the majority of cases, the qualitative effects of both neuronal and perceptual adaptation are the same regardless of duration with the quantitative effects simply increasing over time. For adaptation to low-level stimulus properties such as contrast, intensity, and speed, most tuning changes produced by *modulations* in stimulus statistics are evident within 100–1000 ms (Dean, Robinson, Harper, & McAlpine, 2008; Fairhall, Lewen, Bialek, & de Ruyter van Steveninck, 2001; Nagel & Doupe, 2006). While comparable physiological experiments have not been conducted with dynamically changing direction distributions to characterize direction tuning, the timescales of neuronal adaptation in other systems are consistent with our ability to observe perceptual changes in direction discrimination performance after 1500-ms adaptation. Further, a recent report has demonstrated that motion aftereffects can be produced in response to just tens of milliseconds of motion adaptation (Glasser et al., 2011), demonstrating that the individual motion periods used in our stimulus are effective at causing adaptation. At this stage, no study has definitively linked perceptual and neuronal adaptation to stimulus statistics; however, our stimulus and task will allow the simultaneous measurement of perceptual sensitivity and neuronal sensitivity using reverse correlation.

A significant limitation of our model and psychophysical stimulus is that only fixed-frame durations of 10 ms were examined with the overall effects of adaptation modeled only by the distribution of directions throughout the adaptation period. Thus, stimuli at the start and end of the adaptation period were assumed to have equivalent effects on perception of the test. Further, the model assumes that a stimulus alternating direction every 100 ms would have the same effect as one alternating every 10 ms or 0.1 ms because the direction probability distribution is the same in each case. Psychophysical reverse correlation experiments with a stimulus similar to ours suggest that a complex interaction of short-term facilitation and long-term suppression occurs between frames with the same direction (Iyer et al., 2011). Specifically, detection of a target direction is facilitated for ~ 100 ms after that direction is presented, but suppressed from ~ 100–500 ms after that direction is shown. This combination of facilitation and suppression, together with results from physiological reverse correlation showing nonlinear interactions between adjacent motion frames (Perge et al., 2005), suggests that the effects of our adaptation stimuli are not as straightforward as we have assumed by presenting only the direction probabilities averaged across the entire adaptation period. Fortunately, it is clear that motion information in a single frame can be incorporated perceptually against a noisy background lasting hundreds of milliseconds (Iyer et al., 2011). Further, by averaging the responses of adaptation across many trials, we effectively cancel out any small variations that may occur in the direction perception due to small differences in the sequence of stimulus directions on any single trial. By incorporating the previously reported temporal interactions between successive frames of motion, our model should be able to account for some of the perceptual variability that arises between trials with different adaptation sequences or between trials with different adaptation durations.

Adaptation to stimulus statistics

Previous physiological studies have suggested that sensory neurons adapt so that their range of stimulus sensitivity matches the prevailing stimulus statistics (Barlow, 1961; Laughlin, 1981). The perceptual outcome of these changes should be improved discrimination performance for stimuli within the prevailing distribution, and this has been observed for the discrimination of interaural level differences used to localize sounds (Dahmen et al., 2010). In our experiments, similar neuronal adaptation would predict that the best performance (lowest discrimination thresholds) would occur after adaptation to a single direction with broader direction distributions associated with worse performance. However, we observed no significant effects of adaptation to a symmetric range of directions centered on the category boundary, even when the adaptation conditions were blocked, and the best discrimination performance actually followed the *No Flanks* adaptation condition, which comprised mainly directions with a downward component. Our modeling results support our failure to observe any perceptual changes associated with the range of adaptation direction.

It is possible that differences in the tuning of neurons that contribute to a perceptual judgment may account for the differences between our results and those of Dahmen et al. (2010). Physiological studies demonstrating the matching of neuronal sensitivity to stimulus statistics have focused on neurons with monotonic tuning across the range of tested stimulus attributes.

This is evident in studies of fly H1 sensitivity to low speeds (Brenner, Bialek, & de Ruyter van Steveninck, 2000; Fairhall et al., 2001), sensitivity to sound intensity in inferior colliculus and songbird field L (Dean, Harper, & McAlpine, 2005; Nagel & Doupe, 2006), whisker motion coding in rodent barrel cortex (Maravall et al., 2007), and many studies of luminance and contrast coding in the retina and LGN (Mante et al., 2005; Smirnakis et al., 1997; Wark, Fairhall, & Rieke, 2009). Such monotonic tuning lends itself to efficient coding, in which a fixed dynamic range of neuronal spike rates can be remapped so that all spike rates are equally likely given any stimulus probability distribution (Barlow, 1961; Laughlin, 1981). This efficient coding is readily achieved by shifting the neuron's tuning curve laterally to match the mean stimulus and changing the slope of the tuning curve to incorporate the stimulus variability. Such changes allow a neuron to optimally contribute to discrimination or identification of stimuli within the prevailing distribution, a phenomenon most clearly demonstrated in the retina (Sakmann & Creutzfeldt, 1969).

However, the shape of a neuron's tuning curve may reflect an optimization not just for representing the stimulus statistics but also for executing a range of stimulus-driven behaviors (Salinas, 2006). The neurons that most likely contribute to direction discrimination are those in area MT, which have nonmonotonic, unimodal tuning curves. For stimulus qualities encoded nonmonotonically in a neuron's firing rate, the optimal tuning curve depends on whether the neuron's output will be used for detecting, discriminating, or identifying stimuli (Butts & Goldman, 2006). Further, there is no unique way to optimize a nonmonotonic neuron's tuning curve solely for discrimination, as there are two flanks of the tuning curve that could be matched to the stimulus distribution. Thus it is possible that the ability of sensory systems to engage in optimal inference and match their range of sensitivity to the prevailing stimulus statistics may depend on the associated neurons having monotonic tuning curves.

While the different roles of unimodal and monotonic tuning curves (or value versus intensity coding) remain unclear, unimodal tuning curves are common in neurons that encode spatially related qualities such as orientation, direction, speed, and position. If adaptation-induced lateral shifts in the tuning of such neurons does not or cannot specifically subserve efficient encoding to allow optimal stimulus detection or discrimination, adaptation-induced gain changes may improve other behaviors such as the ability to detect stimulus changes. Adaptation of unimodal neurons may also enhance the ability to represent multiple simultaneous stimulus values or a single, rapidly changing stimulus value, as is required for accurate trajectory estimation and object tracking.

Acknowledgments

This work was supported by a Human Frontier Science Program Career Development Award, an Establishment Award from the Ramaciotti Foundation, and Australian NHMRC Project Grant 1008287.

Commercial relationships: none.
Corresponding author: Nicholas S. C. Price.
Email: nicholas.price@monash.edu
Address: Department of Physiology, Monash University, Clayton, Victoria, Australia.

References

Bair, W., & Movshon, J. A. (2004). Adaptive temporal integration of motion in direction-selective neurons in macaque visual cortex. *Journal of Neuroscience, 24*(33), 7305–7323.

Barlow, H. B. (1961). Chapter 13. Possible principles underlying the transformations of sensory messages. In Rosenblith, W. (Ed.), *Sensory Communication*. (pp. 217–234): MIT Press.

Bex, P. J., Bedingham, S., & Hammett, S. T. (1999). Apparent speed and speed sensitivity during adaptation to motion. *Journal of the Optical Society of America a-Optics Image Science and Vision, 16*(12), 2817–2824.

Bonds, A. B. (1989). Role of inhibition in the specification of orientation selectivity of cells in the cat striate cortex. *Visual Neuroscience, 2*(1), 41–55.

Borghuis, B. G., Perge, J. A., Vajda, I., van Wezel, R. J., van de Grind, W. A., & Lankheet, M. J. (2003). The motion reverse correlation (MRC) method: a linear systems approach in the motion domain. *Journal of Neuroscience Methods, 123*(2), 153–166.

Brainard, D. H. (1997). The Psychophysics Toolbox. *Spatial Vision, 10*(4), 433–436.

Brenner, N., Bialek, W., & de Ruyter van Steveninck, R. R. (2000). Adaptive rescaling maximizes information transmission. *Neuron, 26*, 695–702.

Britten, K. H., & Newsome, W. T. (1998). Tuning bandwidths for near-threshold stimuli in area MT. *Journal of Neurophysiology, 80*(2), 762–770.

Britten, K. H., Newsome, W. T., Shadlen, M. N., Celebrini, S., & Movshon, J. A. (1996). A relationship between behavioral choice and the visual responses of neurons in macaque MT. *Visual Neuroscience, 13*(1), 87–100.

Buracas, G. T., Zador, A. M., DeWeese, M. R., &

Albright, T. D. (1998). Efficient discrimination of temporal patterns by motion-sensitive neurons in primate visual cortex. *Neuron, 20*(5), 959–969.

Butts, D. A., & Goldman, M. S. (2006). Tuning curves, neuronal variability, and sensory coding. *PLoS Biology, 4*(4), e92.

Clifford, C. W., Webster, M. A., Stanley, G. B., Stocker, A. A., Kohn, A., Sharpee, T. O., & Schwartz, O. (2007). Visual adaptation: neural, psychological and computational aspects. *Vision Research, 47*(25), 3125–3131.

Clifford, C. W. G., & Langley, K. (1996). Psychophysics of motion adaptation parallels insect electrophysiology. *Current Biology, 6*(10), 1340–1342.

Clifford, C. W. G., Wyatt, A. M., Arnold, D. H., Smith, S. T., & Wenderoth, P. (2001). Orthogonal adaptation improves orientation discrimination. *Vision Research, 41*(2), 151–159.

Crowder, N. A., Price, N. S., Hietanen, M. A., Dreher, B., Clifford, C. W., & Ibbotson, M. R. (2006). Relationship between contrast adaptation and orientation tuning in V1 and V2 of cat visual cortex. *Journal of Neurophysiology, 95*(1), 271–283.

Curran, W., Clifford, C. W., & Benton, C. P. (2006). The direction aftereffect is driven by adaptation of local motion detectors. *Vision Research, 46*(25), 4270–4278.

Dahmen, J. C., Keating, P., Nodal, F. R., Schulz, A. L., & King, A. J. (2010). Adaptation to stimulus statistics in the perception and neural representation of auditory space. *Neuron, 66*(6), 937–948.

Dean, I., Harper, N. S., & McAlpine, D. (2005). Neural population coding of sound level adapts to stimulus statistics. *Nature Neuroscience, 8*(12), 1684–1689.

Dean, I., Robinson, B. L., Harper, N. S., & McAlpine, D. (2008). Rapid neural adaptation to sound level statistics. *Journal of Neuroscience, 28*(25), 6430–6438.

Dragoi, V., Sharma, J., & Sur, M. (2000). Adaptation-induced plasticity of orientation tuning in adult visual cortex. *Neuron, 28*(1), 287–298.

Fairhall, A. L., Lewen, G. D., Bialek, W., & de Ruyter van Steveninck, R. R. (2001). Efficiency and ambiguity in an adaptive neural code. *Nature, 412*, 787–792.

Felsen, G., Shen, Y. S., Yao, H., Spor, G., Li, C., & Dan, Y. (2002). Dynamic modification of cortical orientation tuning mediated by recurrent connections. [Research Support, U.S. Gov't, Non-P.H.S. Research Support, U.S. Gov't, P.H.S.]. *Neuron, 36*(5), 945–954.

Gibson, J. J., & Radner, M. (1937). Adaptation, after-effect and contrast in the perception of tilted lines. I. Quantitative studies. *Journal of Experimental Psychology, 20*(5), 453–467.

Gilbert, C. D., & Wiesel, T. N. (1990). The influence of contextual stimuli on the orientation selectivity of cells in primary visual cortex of the cat. *Vision Research, 30*(11), 1689–1701.

Glasser, D. M., Tsui, J. M., Pack, C. C., & Tadin, D. (2011). Perceptual and neural consequences of rapid motion adaptation. *Proceedings of the National Academy of Sciences of the United States of America, 108*(45), E1080–1088. doi: 10.1073/pnas.1101141108.

Graf, A. B., Kohn, A., Jazayeri, M., & Movshon, J. A. (2011). Decoding the activity of neuronal populations in macaque primary visual cortex. *Nature Neuroscience, 14*(2), 239–245.

Hol, K., & Treue, S. (2001). Different populations of neurons contribute to the detection and discrimination of visual motion. *Vision Research, 41*(6), 685–689.

Iyer, P. B., Freeman, A. W., McDonald, J. S., & Clifford, C. W. (2011). Rapid serial visual presentation of motion: short-term facilitation and long-term suppression. *Journal of Vision, 11*(3)16, 1–14, http://www.journalofvision.org/content/11/3/16, doi: 10.1167/11.3.16. [PubMed] [Article]

Jin, D. Z., Dragoi, V., Sur, M., & Seung, H. S. (2005). Tilt aftereffect and adaptation-induced changes in orientation tuning in visual cortex. *Journal of Neurophysiology, 94*(6):4038–4050. doi: 10.1152/jn.00571.2004.

Kohn, A. (2007). Visual adaptation: physiology, mechanisms, and functional benefits. *Journal of Neurophysiology, 97*(5), 3155–3164.

Kohn, A., & Movshon, J. A. (2003). Neuronal adaptation to visual motion in area MT of the macaque. *Neuron, 39*, 681–691.

Kohn, A., & Movshon, J. A. (2004). Adaptation changes the direction tuning of macaque MT neurons. *Nature Neuroscience, 7*(7), 764–772.

Laughlin, S. (1981). A simple coding procedure enhances a neuron's information capacity. *Zeitschrift für Naturforschung C, 36*(9-10), 910–912.

Levinson, E., & Sekuler, R. (1976). Adaptation alters perceived direction of motion. *Vision Research, 16*(7), 779–781.

Mante, V., Frazor, R. A., Bonin, V., Geisler, W. S., & Carandini, M. (2005). Independence of luminance and contrast in natural scenes and in the early visual system. *Nature Neuroscience, 8*(12), 1690–1697.

Maravall, M., Petersen, R. S., Fairhall, A. L., Arabzadeh, E., & Diamond, M. E. (2007). Shifts in coding properties and maintenance of information transmission during adaptation in barrel cortex. *PLoS Biology, 5*(2), e19.

Morrone, M. C., Burr, D. C., & Maffei, L. (1982). Functional implications of cross-orientation inhibition of cortical visual cells. I. Neurophysiological evidence. *Proceedings of the Royal Society B: Biological Sciences, 216*(1204), 335–354.

Movshon, J. A., Adelson, E. H., Gizzi, M. S., & Newsome, W. T. (1985). The analysis of moving visual patterns. In Chagas, C., Gattass, R. & Gross, C. G. (Eds.), *Pattern recognition mechanisms*. (pp. 117–151). Berlin: Springer-Verlag.

Muller, J. R., Metha, A. B., Krauskopf, J., & Lennie, P. (1999). Rapid adaptation in visual cortex to the structure of images. *Science, 285*(5432), 1405–1408.

Nagel, K. I., & Doupe, A. J. (2006). Temporal processing and adaptation in the songbird auditory forebrain. *Neuron, 51*(6), 845–859.

Newsome, W. T., Britten, K. H., & Movshon, J. A. (1989). Neuronal correlates of a perceptual decision. *Nature, 341*(6237), 52–54.

Newsome, W. T., & Pare, E. B. (1988). A selective impairment of motion perception following lesions of the middle temporal visual area (MT). *Journal of Neuroscience, 8*(6), 2201–2211.

Pelli, D. G. (1997). The VideoToolbox software for visual psychophysics: transforming numbers into movies. *Spatial Vision, 10*(4), 437–442.

Perge, J. A., Borghuis, B. G., Bours, R. J., Lankheet, M. J., & van Wezel, R. J. (2005). Temporal dynamics of direction tuning in motion-sensitive macaque area MT. *Journal of Neurophysiology, 93*(4), 2104–2116. doi: 10.1152/jn.00601.2004.

Petersen, S. E., Baker, J. F., & Allman, J. M. (1985). Direction-specific adaptation in area MT of the owl monkey. *Brain Research, 346*(1), 146–150.

Phinney, R. E., Bowd, C., & Patterson, R. (1997). Direction-selective coding of stereoscopic (cyclopean) motion. *Vision Research, 37*(7), 865–869.

Price, N. S., & Born, R. T. (2010). Timescales of sensory- and decision-related activity in the middle temporal and medial superior temporal areas. *Journal of Neuroscience, 30*(42), 14036–14045. doi: 10.1523/JNEUROSCI.2336-10.2010.

Price, N. S., Ibbotson, M. R., Ono, S., & Mustari, M. J. (2005). Rapid processing of retinal slip during saccades in macaque area MT. *Journal of Neurophysiology, 94*(1), 235–246.

Priebe, N. J., Churchland, M. M., & Lisberger, S. G. (2002). Constraints on the source of short-term motion adaptation in macaque area MT. I. the role of input and intrinsic mechanisms. *Journal of Neurophysiology, 88*(1), 354–369.

Priebe, N. J., & Lisberger, S. G. (2002). Constraints on the source of short-term motion adaptation in macaque area MT. II. tuning of neural circuit mechanisms. *Journal of Neurophysiology, 88*(1), 370–382.

Raymond, J. E. (1993). Movement direction analysers: independence and bandwidth. *Vision Research, 33*(5-6), 767–775.

Sakmann, B., & Creutzfeldt, O. D. (1969). Scotopic and mesopic light adaptation in the cat's retina. *Pflugers Arch, 313*(2), 168–185.

Salinas, E. (2006). How behavioral constraints may determine optimal sensory representations. *PLoS Biology, 4*(12), e387.

Salzman, C. D., Britten, K. H., & Newsome, W. T. (1990). Cortical microstimulation influences perceptual judgements of motion direction. *Nature, 346*(6280), 174–177.

Saul, A. B., & Cynader, M. S. (1989a). Adaptation in single units in visual cortex: the tuning of aftereffects in the spatial domain. *Visual Neuroscience, 2*, 593–607.

Saul, A. B., & Cynader, M. S. (1989b). Adaptation in single units in visual cortex: the tuning of aftereffects in the temporal domain. *Visual Neuroscience, 2*(6), 609–620.

Schrater, P. R., & Simoncelli, E. P. (1998). Local velocity representation: evidence from motion adaptation. *Vision Research, 38*(24), 3899–3912.

Sheth, B. R., Ventura, G., & Wu, D. A. (2009). Does adaptation of motion-direction detectors affect bias or sensitivity of direction judgments? *Perception, 38*(11), 1621–1627.

Simoncelli, E. P., & Heeger, D. J. (1998). A model of neuronal responses in visual area MT. *Vision Research, 38*(5), 743–761.

Smirnakis, S. M., Berry, M. J., Warland, D. K., Bialek, W., & Meister, M. (1997). Adaptation of retinal processing to image contrast and spatial scale. *Nature, 386*(6620), 69–73.

Snowden, R. J., Treue, S., Erickson, R. G., & Andersen, R. A. (1991). The response of area MT and V1 neurons to transparent motion. *Journal of Neuroscience, 11*(9), 2768–2785.

Teich, A. F., & Qian, N. (2003). Learning and adaptation in a recurrent model of V1 orientation selectivity. *Journal of Neurophysiology, 89*(4), 2086–2100.

Treue, S., Hol, K., & Rauber, H. J. (2000). Seeing

multiple directions of motion-physiology and psychophysics. *Nature Neuroscience, 3*(3), 270–276.

Troje, N. F., Sadr, J., Geyer, H., & Nakayama, K. (2006). Adaptation aftereffects in the perception of gender from biological motion. *Journal of Vision, 6*(8):7, 850–857, http://www.journalofvision.org/content/6/8/7, doi: 10.1167/6.8.7. [PubMed] [Article]

Van Wezel, R. J., & Britten, K. H. (2002). Motion adaptation in area MT. *Journal of Neurophysiology, 88*(6), 3469–3476. doi: 10.1152/jn.00276.2002.

Wark, B., Fairhall, A., & Rieke, F. (2009). Timescales of inference in visual adaptation. *Neuron, 61*(5), 750–761.

Watamaniuk, S. N., Sekuler, R., & Williams, D. W. (1989). Direction perception in complex dynamic displays: the integration of direction information. *Vision Research, 29*(1), 47–59.

Webster, M. A., Kaping, D., Mizokami, Y., & Duhamel, P. (2004). Adaptation to natural facial categories. *Nature, 428*(6982), 557–561.

Wenderoth, P., & Wiese, M. (2008). Retinotopic encoding of the direction aftereffect. *Vision Research, 48*(19), 1949–1954.

Williams, D. W., & Sekuler, R. (1984). Coherent global motion percepts from stochastic local motions. *Vision Research, 24*(1), 55–62.

Yang, J., & Lisberger, S. G. (2009). Relationship Between Adapted Neural Population Responses in MT and Motion Adaptation in Speed and Direction of Smooth-Pursuit Eye Movements. *Journal of Neurophysiology, 101*(5), 2693–2707.